

Title	Vascular branching point counts using photoacoustic imaging in the superficial layer of the breast: A potential biomarker for breast cancer
Author(s)	Yamaga, Iku; Kawaguchi-Sakita, Nobuko; Asao, Yasufumi; Matsumoto, Yoshiaki; Yoshikawa, Aya; Fukui, Toshifumi; Takada, Masahiro; Kataoka, Masako; Kawashima, Masahiro; Fakhrejehani, Elham; Kanao, Shotaro; Nakayama, Yoshie; Tokiwa, Mariko; Torii, Masae; Yagi, Takayuki; Sakurai, Takaki; Haga, Hironori; Togashi, Kaori; Shiina, Tsuyoshi; Toi, Masakazu
Citation	Photoacoustics (2018), 11: 6-13
Issue Date	2018-09
URL	<a href="http://hdl.handle.net/2433/234594">http://hdl.handle.net/2433/234594</a>
Right	© 2018 The Authors. Published by Elsevier GmbH. This is an open access article under the CC BY-NC-ND license ( <a href="http://creativecommons.org/licenses/by-nc-nd/4.0/">http://creativecommons.org/licenses/by-nc-nd/4.0/</a> ).
Type	Journal Article
Textversion	publisher



ELSEVIER

Contents lists available at ScienceDirect

## Photoacoustics

journal homepage: [www.elsevier.com/locate/pacs](http://www.elsevier.com/locate/pacs)

## Research article

# Vascular branching point counts using photoacoustic imaging in the superficial layer of the breast: A potential biomarker for breast cancer



Iku Yamaga<sup>a</sup>, Nobuko Kawaguchi-Sakita<sup>b</sup>, Yasufumi Asao<sup>c</sup>, Yoshiaki Matsumoto<sup>a</sup>, Aya Yoshikawa<sup>a</sup>, Toshifumi Fukui<sup>d</sup>, Masahiro Takada<sup>a</sup>, Masako Kataoka<sup>e</sup>, Masahiro Kawashima<sup>a</sup>, Elham Fakhrehani<sup>f</sup>, Shotaro Kanao<sup>e</sup>, Yoshie Nakayama<sup>a</sup>, Mariko Tokiwa<sup>a</sup>, Masae Torii<sup>a</sup>, Takayuki Yagi<sup>c</sup>, Takaki Sakurai<sup>g</sup>, Hironori Haga<sup>g</sup>, Kaori Togashi<sup>e</sup>, Tsuyoshi Shiina<sup>h</sup>, Masakazu Toi<sup>a,\*</sup>

<sup>a</sup> Department of Breast Surgery, Graduate School of Medicine, Kyoto University, Japan

<sup>b</sup> Department of Clinical Oncology, Kyoto University Hospital, Japan

<sup>c</sup> Japan Science and Technology Agency, Japan

<sup>d</sup> Medical Imaging System Development Center, Canon Inc., Japan

<sup>e</sup> Department of Diagnostic Imaging and Nuclear Medicine, Graduate School of Medicine, Kyoto University, Japan

<sup>f</sup> Kyoto Breast Cancer Research Network Organization, Japan

<sup>g</sup> Department of Diagnostic Pathology, Graduate School of Medicine, Kyoto University, Japan

<sup>h</sup> Department of Human Health Science, Graduate School of Medicine, Kyoto University, Japan

## ARTICLE INFO

## Keywords:

Biomarker  
Breast cancer  
Photoacoustic imaging  
Vasculature  
Vessel branching points

## ABSTRACT

This study aimed to identify the characteristics of the vascular network in the superficial subcutaneous layer of the breast and to analyze differences between breasts with cancer and contralateral unaffected breasts using vessel branching points (VBPs) detected by three-dimensional photoacoustic imaging with a hemispherical detector array. In 22 patients with unilateral breast cancer, the average VBP counts to a depth of 7 mm below the skin surface were significantly greater in breasts with cancer than in the contralateral unaffected breasts ( $p < 0.01$ ). The ratio of the VBP count in the breasts with cancer to that in the contralateral breasts was significantly increased in patients with a high histologic grade ( $p = 0.03$ ), those with estrogen receptor-negative disease ( $p < 0.01$ ), and those with highly proliferative disease ( $p < 0.01$ ). These preliminary findings indicate that a higher number of VBPs in the superficial subcutaneous layer of the breast might be a biomarker for primary breast cancer.

## 1. Introduction

Ultrasonography (US), mammography, magnetic resonance imaging (MRI), computed tomography and positron emission tomography are used to diagnose breast cancer based on the morphology and properties of the tumor [1]. Features of tumor-associated blood vessels have been reported not only to be intratumoral such as tumor angiogenesis [2], but also to include the vascular architecture around the tumor [3,4]. The modalities presently available for imaging of the vasculature include Doppler US, contrast-enhanced US, and contrast-enhanced MRI [3,5–9]. However, the contrast agents used can cause allergic reactions and agents such as gadolinium cannot be used in patients with severe renal dysfunction. Diffuse optical tomography using near-infrared light

can measure the amount of water, fat, and total hemoglobin as well as its oxygen saturation in tissues [10]. These parameters do not require a contrast agent and can be measured noninvasively. However, the resolution is in the order of centimeters, so it is difficult to discriminate tumor tissue from normal breast tissue when the tumor is less than a few centimeters in size. Tumor-related vascular changes in the superficial layer of breasts had not been reported in detail. Photoacoustic imaging provides good visualization of these superficial areas, and is able to highlight changes in the superficial vasculature due to tumor.

We have developed a photoacoustic imaging (PAI) system for assessment of blood vessels [4,11–13]. The third iteration of our prototype system (PAI-03) has high performance to a depth of more than 20 mm from the skin surface with submillimeter resolution, allowing

*Abbreviations:* BP, blood pressure; DCIS, ductal carcinoma in situ; HDA, hemispherical detector array; MRI, magnetic resonance imaging; PAI, photoacoustic imaging; US, ultrasonography; VBP, vessel branching point

\* Corresponding author.

E-mail address: [toi@kuhp.kyoto-u.ac.jp](mailto:toi@kuhp.kyoto-u.ac.jp) (M. Toi).

<https://doi.org/10.1016/j.pacs.2018.06.002>

Received 31 December 2017; Received in revised form 27 May 2018; Accepted 11 June 2018

Available online 20 June 2018

2213-5979/ © 2018 The Authors. Published by Elsevier GmbH. This is an open access article under the CC BY-NC-ND license

(<http://creativecommons.org/licenses/by-nc-nd/4.0/>).

the structure of fine blood vessels to be visualized [4]. Use of a hemispherical detector array (HDA) and three-dimensional constructed images provides detailed images of the vascular structures. We have successfully used the PAI-03 system to detect and analyze blood vessels associated with cancer.

The PAI system can visualize the vascular network of the breast as well as the tumor-related vasculature with high resolution. In a previous study using the PAI-03 system, we identified certain features of cancer-associated blood vessels [4]. Adjacent blood vessels oriented toward the tumor were visualized in patients with invasive breast cancer, and photoacoustic signals were found to be increased in the tumor in some cases that had received preoperative chemotherapy. Tumor angiogenesis results in the formation of immature blood vessels, which increases the vascular permeability [2]. Increased vascular permeability elevates the interstitial pressure and stagnates blood flow, despite the increase in metabolism and the blood flow requirements [2,14]. Therefore, we hypothesized that blood volume around the tumor including the subcutaneous layer might be increased due to the influence of increase blood flow requirements on the tumor.

We have been using this system in patients with breast cancer to evaluate the characteristics of the vascular network in the breast in detail, including vessel branching points (VBPs) in both the superficial area just below the skin surface and in the whole breast within the visual range. In this study, VBPs were defined as the points where blood vessels divide into two or more branches. We have been attempting to detect differences in blood flow between breasts with cancer and contralateral breasts with no detectable cancer using the number of visible VBPs.

In this report, we present our preliminary data on the relationship between VBP counts in breasts with cancer and those in contralateral breasts with no detectable cancer to determine the potential utility of VBP as a biomarker of primary breast cancer.

## 2. Material and methods

### 2.1. Patients

Data of 22 patients with unilateral breast cancer who had participated in another clinical trial (UMIN00012251) were analyzed in this study. Patients were enrolled in the clinical trial between December 2014 and December 2015 at Kyoto University Hospital, Japan. The inclusion criteria for the clinical trial were a primary breast lesion, age 20 years or older at the time of diagnosis, and an Eastern Cooperative Oncology Group performance status of 0 or 1. The exclusion criteria included pregnancy, cardiac pacemaker implantation, and any other condition judged by the clinical investigators to make the patient unsuitable for inclusion. Patients with benign lesions were also excluded. The contralateral breasts were diagnosed as cancer-free by mammography, US, and MRI. The study was approved by the institutional review board at Kyoto University (UMIN00012251) and was conducted in accordance with the Helsinki Declaration of 1975, as revised in 2008. All participants provided written informed consent.

### 2.2. Configuration of the PAI system

The VBPs were counted using a PAI-03 system with an HDA (Canon Inc., Tokyo, Japan; in collaboration with Optosonics Inc., Oriental, NC) [4,15]. The system was modified by reducing the depth of the breast-holding cup from 50 mm to 38 mm. A laser capable of irradiating at wavelengths of 755 nm and 795 nm was also used. The detector array was scanned continuously in a spiral pattern in one plane. The spiral scanning pattern was modified to gradually increase the density of data acquisition points as the scan approached the center of the spiral scan. AQ-switched alexandrite laser with selectable wavelengths of 755 nm and 795 nm was used. The laser energy used in the PAI-03 system is approximately 200 mJ/pulse and is constant for both wavelengths. The

light illumination was 60 mm in diameter at the surface of the breast cup. The maximum light energy was set to less than 10 mJ/cm<sup>2</sup>, which is half the maximum permissible exposure recommended by the American National Standards Institute.

A piezoelectric zirconate titanate transducer was used to detect the PA signal. The HDA used contains 512 elements on its internal surface, each within a circle measuring 3 mm in diameter. The central frequency was 2 MHz. The imaging area for each laser shot was just within the range of the 30-mm radius of the cylinder. To enhance the imaging area, the HDA was scanned spirally in the horizontal plane; this allowed the imaging area to be selected at radii of 50 mm, 70 mm, and 100 mm. For each scan data acquisition was set to at either 1024 or 2048 corresponding to an acquisition time of 51.2 s and 102.4 s, respectively. Using a spherical phantom with a diameter of 0.3 mm, the full width at half maximum was 0.57 mm in the x and y directions and 0.37 mm in the z direction.

### 2.3. Acquisition of PAI data

For each patient, both breasts were scanned in water at body temperature, first at a wavelength of 795 nm and then at a wavelength of 755 nm. In each case, a PA image acquired at 795 nm that had equal oxyhemoglobin and deoxyhemoglobin absorption coefficients and the image corresponding to the total hemoglobin distribution were used to analyze the structure of the blood vessels. Hemoglobin oxygen saturation was not analyzed, so the images taken at a wavelength of 755 nm were not used. PA images were reconstructed using a universal back-projection algorithm [16], taking into account the average speed of sound in breast tissue and that in water for impedance matching. The variations in light fluence in tissue from patient to patient were compensated for by calculating the result of the diffusion equation. The PAI images in this study were constructed using the absorption coefficient at 795 nm and the color signal intensity.

### 2.4. Extraction of the breast surface data

A PAI image of the breast in the coronal plane was used to extract the breast surface. The areas where the skin pigment signal started were contoured, and the plotted points were obtained manually at intervals of about 1–2 cm per slice of a 2D image. The same contour extraction procedure was performed for slices at least every 10 slices (1.25 mm) to obtain a three-dimensional breast contour point group. When the deviation between the spline curve based on the original plot points and the breast shape by skin pigment signal was more than 3 mm, the contour was extracted by adding more plot points. Typically, there were 200–300 plot points per breast. The surface shape of the breast was reconstructed by approximating these contours as a curved surface. The moving least squares method [17] was used for surface approximation.

### 2.5. MRI data acquisition

Breast MRI was performed using a 3.0-T scanner (MAGNETOM Trio, A Tim System, Siemens AG, Germany) with a dedicated 16-channel breast array coil. Fat-suppressed T1-weighted dynamic contrast-enhanced images were obtained pre-contrast and then at 1–2 min (early) and 5–6 min (delayed) after gadolinium injection. Gadoteridol (ProHance, Eisai Inc., Tokyo, Japan) was power-injected at a dose of 0.2 mL/kg and a speed of 2.0 mL/s, then flushed with 20 mL of saline at the same rate. Whole-breast axial scanning at a high temporal resolution was performed for 1 min (3D-VIBE: TR/TE 3.70/1.36 ms, FA 15 and FOV 330 mm × 330 mm, matrix 384 × 346, thickness 1.0 mm). Subtraction images were computed pixelwise by subtracting the signal intensity of the pre-contrast images from that of the early post-contrast images.

Deformed MRI images were constructed based on pre-contrast and early post-contrast MRI subtraction images in which blood vessels could

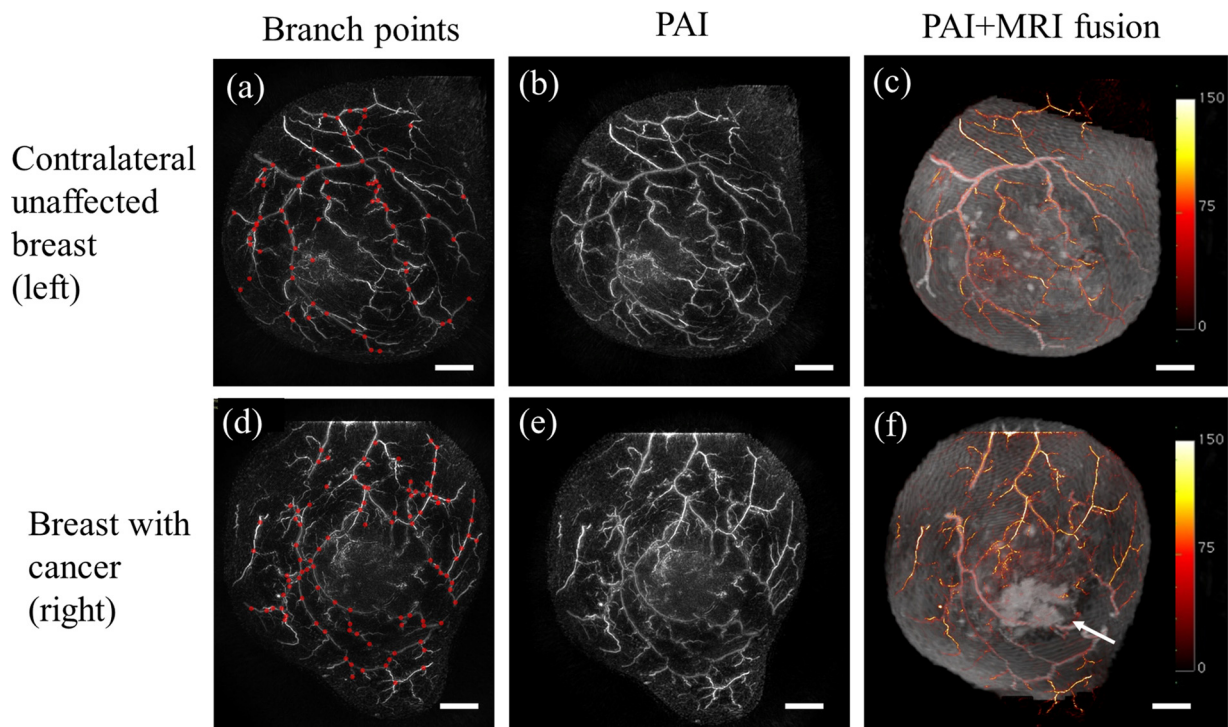


**Fig. 1.** (a, d) Number of branching points in a breast with cancer and the contralateral breast with no detectable cancer. Points counted on the PAI image are shown in red. (b, e) PAI image. (c, f) Color PAI image with deformed MRI. The arrow indicates the site of the cancer. The color bar represents the PAI signal amplitude. Scale bar, 20 mm. MRI, magnetic resonance imaging; PAI, photoacoustic imaging.

be observed as with PAI. We manually identified common features, such as VBPs or intermediate points between branch and branch in both modalities, referred to here as “corresponding points”. We then deformed the whole breast shape in three dimensions to match each corresponding point using the thin plate spline method [18].

## 2.6. Counting methodology

Evaluation was carried out using the signal intensity of PAI images obtained at a wavelength of 795 nm and deformed MRI subtraction images. The blood vessels with corresponding points on the MRI image were defined as “corresponding vessels”. VBPs in the PAI image were defined as the branching points on these corresponding vessels (Fig. 1). The entire PAI image was defined as the area of interest. Three independent observers (one was a breast surgeon, and the others were image processing specialists) manually counted the number of branches on the corresponding vessels in the three-dimensional image acquired by PAI. Blood vessel branches other than those of the corresponding vessels detected on the PAI image were excluded from the analysis. The branching density values (count per  $100\text{ cm}^2$ ) were calculated after normalizing the VBPs to the surface area in the region of interest.

## 2.7. Clinicopathologic characteristics

The patients’ medical records were reviewed to obtain clinicopathologic data on age, menopausal status, presence of cardiovascular disease, smoking history, lactation history, hemoglobin status, body mass index, and systolic blood pressure (BP) at the time of PAI. Tumor diameter and nodal status were determined based on the pathology reports for the surgical specimens.

After surgery, the excised specimens were sectioned at 5-mm intervals perpendicular to the longest axis of the specimen. The pathologic analysis was performed in a conventional manner using formalin-fixed, paraffin-embedded tissues stained with hematoxylin-eosin. Estrogen and progesterone receptor status in cases of invasive

carcinoma was confirmed by immunohistochemistry. HER2 status was confirmed by immunohistochemistry or fluorescent in situ hybridization. Ki-67 immunostaining was performed using the MIB1 monoclonal antibody (Dako, Copenhagen, Denmark). Histologic grade was determined by experienced breast pathologists according to the General Rules for Clinical and Pathological Recoding of Breast Cancer, 15<sup>th</sup> edition, based on scores for nuclear pleomorphism, tubule formation, and mitotic count.

## 2.8. Statistical analysis

All statistical analyses were performed using JMP 12.2.0 for Windows (SAS Institute Inc., Cary, NC). The Wilcoxon signed-rank test was used to detect differences in VBP counts between breasts with cancer and the contralateral unaffected breasts. The Wilcoxon rank-sum test was used to determine the relationship between each clinicopathologic parameter and the VBP count on each side. A  $p$ -value  $< 0.05$  was considered statistically significant.

## 3. Results

### 3.1. Patient characteristics and histologic diagnoses

Data for 22 patients with breast cancer were analyzed. The patient characteristics and the histopathologic characteristics of the breast cancers are shown in Table 1. Seven patients had cardiovascular disease, 3 of whom were on antihypertensive treatment with a calcium channel blocker ( $n = 2$ ) or an angiotensin-converting enzyme inhibitor ( $n = 1$ ); both these classes of agents exert their antihypertensive effect by vasodilation. The breast lesions were diagnosed as ductal carcinoma in situ (DCIS) in 3 patients and invasive carcinoma in 19 patients.

### 3.2. Analysis of vessel branching points

Fig. 2 shows a comparison of the VBP counts between MRI and PAI

**Table 1**  
Characteristics of patients and breast cancers.

Mean age, years	51.5 (34–74)
Menopausal status,	
Premenopausal/Perimenopausal, n	12
Postmenopausal, n	10
Medical history	
Cardiovascular disease	7
Antihypertensive drugs	3
Smoking	6
Lactation history	13
Mean body mass index (kg/m <sup>2</sup> )	24.2 (19.8–35.9)
Mean systolic blood pressure	119.2 (92–155)
Mean hemoglobin level (mg/mL)	13.1 (7.0–14.5)
Ductal carcinoma in situ	3
Invasive carcinoma	19
T	
1	7
2	9
3	2
4	1
N	
0	12
1	6
2	1
3	0
M	
0	18
1	1
Estrogen receptor status	
Positive	15
Negative	4
HER2 status	
Positive	3
Negative	16
Histologic grade	
1	9
2	2
3	8
Median Ki-67 index (%)	15.9

based on the MRI images. The counting area was within a 20-mm radius of the nipple and to a depth of 5 mm. The median number of VBPs was 18 (range, 8–42)/area on PAI and 2 (range, 0–9)/area on MRI. The difference was statistically significant ( $p < 0.01$ , Wilcoxon signed-rank test).

The distribution of the VBPs is shown in Fig. 3. The focus in this study was the superficial area, so the analyses were performed for data to a depth of 7 mm below the skin surface, where high-resolution images of the vascular network could be captured stably for the whole breast in a measuring cup as described previously [4].

The VBP counts were significantly higher in the breasts with cancer

than in the contralateral unaffected breasts ( $p < 0.01$ , Wilcoxon signed-rank test; Fig. 4). The median VBP counts were 31.7 (range, 5.87–67.0)/100 cm<sup>2</sup> in the breasts with cancer and 27.0 (range, 6.40–44.4)/100 cm<sup>2</sup> on the contralateral side. Differences in the VBP count between the affected and unaffected breasts at depths of 1 mm, 3 mm, and 5 mm, as well as for the whole breast, were all statistically significant ( $p < 0.01$ ) and remained so after exclusion of the data for patients on vasodilating antihypertensive drugs.

To identify the factors that increased the ratio of the VBP count on the affected side to that on the unaffected side, we examined the relationship between this ratio and the patient and tumor characteristics. The VBP count ratio differed significantly according to histologic grade, estrogen receptor status, and Ki-67 positivity (Table 2). In 4 of 19 cases with invasive breast cancer, the VBP count ratio was less than 1.0; all 4 cases were estrogen receptor-positive and had low Ki-67 values.

There was no significant increase in the VBP count on the affected side in comparison with the unaffected side according to nodal status or whether the disease stage was T1 or T2. There were 3 cases of DCIS, one of which showed a marked increase in the number of VBPs. In one case, there was no difference in the VBP count between the affected and unaffected side, and in the remaining case, the VBP count was higher on the unaffected side.

The VBP counts varied widely from patient to patient. This variation was investigated in relation to patient and tumor characteristics and according to the difference in VBP count between the affected and unaffected sides (Table 3). There was no significant difference in the VBP count on either side according to age, menopausal status, presence of cardiovascular disease, smoking history, lactation history, hemoglobin status, or body mass index. However, the VBP count on the contralateral side was significantly different in patients with systolic BP  $> 130$  mmHg compared with those with systolic BP  $\leq 130$  mmHg; this difference remained when the data were analyzed after exclusion of patients on antihypertensive agents.

#### 4. Discussion

Few studies have assessed the fine vasculature in the superficial tissue of the breast. However, a previous study using contrast-enhanced MRI with gadolinium did not detect any difference in the VBP count between patients with benign breast disease and those with breast cancer [7].

In the present study, more fine vessels were detected by PAI than by MRI. There was a significant difference in the VBP count between breasts with cancer and the contralateral breasts, possibly because of an increase in blood vessel branching and increased blood volume in the affected breasts. Based on the signals, including those from the superficial layers, it was unlikely that angiogenesis occurred. PAI detects signals from red blood cells rather than the vessel walls and VBPs were

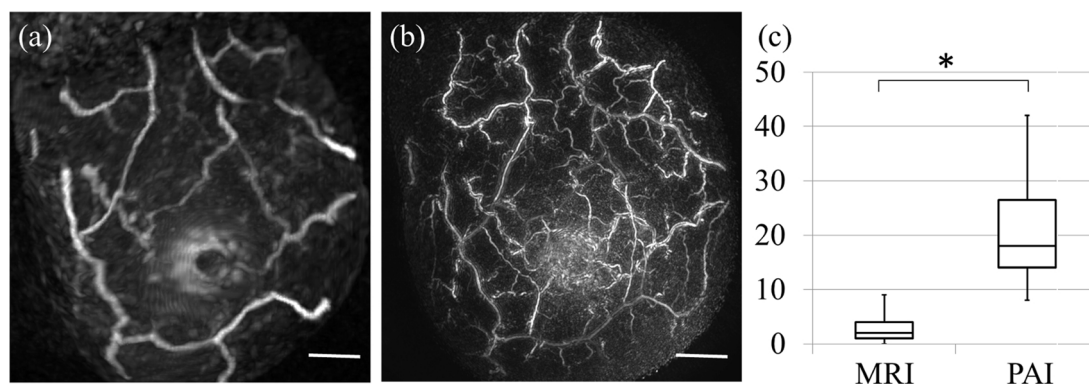


**Fig. 2.** Number of vascular branching points seen on MRI and PAI. (a) Image from a patient with invasive carcinoma acquired by PAI. Scale bar, 20 mm. (b) Image from the same patient acquired by MRI. Scale bar, 20 mm. (c) Comparison of the number of vascular branching points between MRI and PAI based on MRI images. \* $p < 0.01$  (Wilcoxon signed-rank test), MRI, magnetic resonance imaging; PAI, photoacoustic imaging.

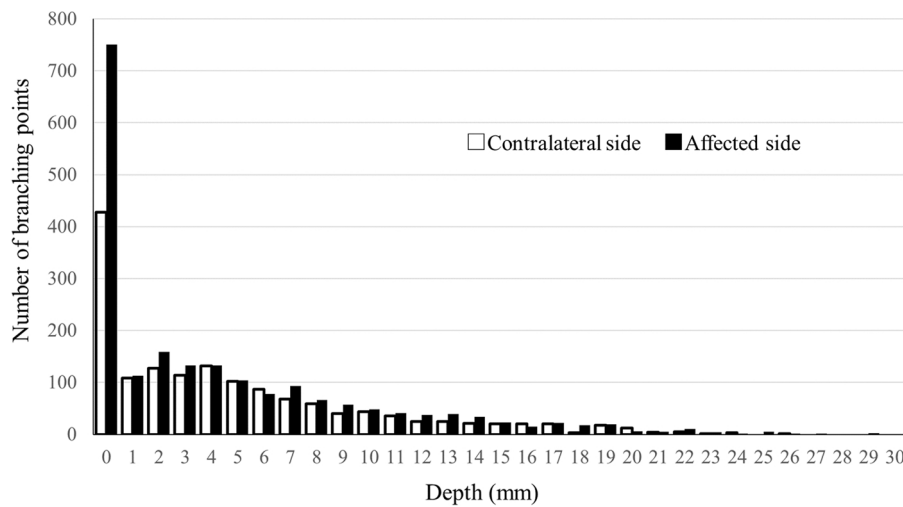


**Fig. 3.** Number of vascular branching points according to depth from the skin surface. (□) Breasts with cancer. (■) Contralateral breasts without cancer. The depth is the distance from extracted surface on photoacoustic imaging.

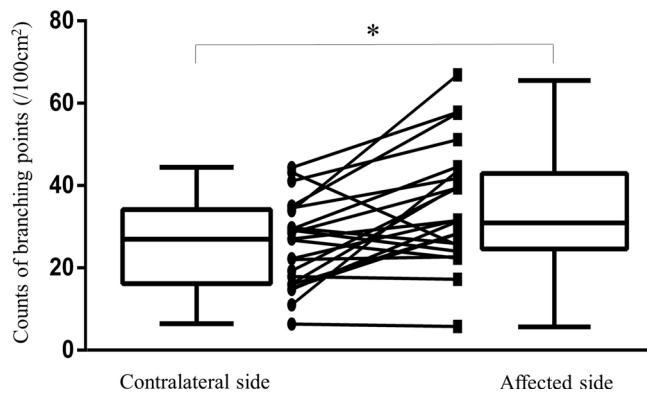


**Fig. 4.** Comparison of the number of vessel branching points in breasts with cancer and in the contralateral breasts without cancer to a depth of 7 mm from the skin surface. \*p < 0.01 (Wilcoxon signed-rank test).

on linear signals considered to be blood vessels, so a change in the VBP count could indicate a change in blood dynamics within the vessels. Our findings suggest that breasts with cancer may contain a greater volume of blood than those without cancer.

The VBP count was higher in breasts with cancer if the Ki-67 index was high and if the cancer had a high histologic grade or was estrogen receptor-negative. These factors generally predict a high proliferation rate and poor prognosis [19,20]. Our findings are consistent with the concept that a tumor needs a blood supply to be able to proliferate, and it will be necessary to investigate the relationship between the VBP count ratio and the prognosis in the future.

The finding of an increase in the blood volume of the whole breast on the affected side may reflect cancer-related upregulation of local metabolic activity [21]. In addition, a high interstitial pressure driven by the tumor may change blood flow around the lesion in terms of not only speed [22] but also volume and may also have an effect in the subcutaneous tissues. Multiple factors are expected to be involved in these changes in blood flow, including energy consumption, interstitial pressure, and vascular permeability [2,19,21,23]. We found a relationship between VBP count and BP, and events associated with high BP may include an increased VBP count in the breast.

Compared with the unaffected sides, the number of VBP counts in affected sides increased in both T1 and T2 cases, and the number of VBP counts also increased in both N negative and N positive cases. the number of VBP count was higher on the affected side than on the contralateral side in 1 out of 3 DCIS cases. On the other hand, some

**Table 2**

Relationship between the ratio of vascular branching points (breast with cancer/contralateral breast) and clinicopathologic factors.

		N	VBP ratio (median)	p-value
Age, years	< 50	10	1.53	0.45
	≥ 50	12	1.27	
Menopausal status	Premenopausal	12	1.53	0.58
	/Perimenopausal			
	Postmenopausal	10	1.27	
Cardiovascular disease	+	7	1.25	0.40
	-	15	1.42	
Antihypertensive medication	+	3	1.25	0.77
	-	19	1.38	
Smoking	+	6	1.84	0.06
	-	16	1.22	
Lactation history	+	13	1.30	0.97
	-	8	1.45	
	Unknown	1		
Body mass index	< 25	16	1.45	0.20
	≥ 25	6	0.99	
Systolic blood pressure	< 130	15	1.42	0.36
	≥ 130	7	1.25	
Hemoglobin (mg/dL)	< 13	5	1.64	0.27
	≥ 13	17	1.3	
Invasion	DCIS	3	1.21	1.00
	Invasive carcinoma	19	1.38	
Tumor size	T1	7	1.51	0.83
	≥ T2	12	1.10	
Nodal metastasis	+	7	1.4	0.47
	-	12	1.17	
Histologic grade	1, 2	11	1.17	0.03*
	3	8	1.82	
ER	+	15	1.25	< 0.01**
	-	4	2.04	
HER2	+	3	1.97	0.11
	-	16	1.27	
Ki-67	< 20	14	1.21	< 0.01**
	≥ 20	5	1.97	

Wilcoxon rank-sum test, \*p < 0.05, \*\*p < 0.01. VBP, vessel branching point.

breasts with cancer showed a decrease in the number of VBPs, and all these cases were estrogen receptor-positive and had low Ki-67 index values. However, this finding is difficult to interpret because of the small number of cases in our study. Further studies in large numbers of patients are needed to elucidate whether PAI is useful for detection of early-stage breast cancer and to identify factors that affect the VBP

**Table 3**  
Relationship between the number of vascular branching points within 7 mm from the skin surface and patient characteristics.

		N	Contralateral side		Tumor side	
			VBP count (median)	p-value	VBP count (median)	p-value
Age, years	< 50	10	20.7	0.20	31.5	0.53
	≥ 50	12	28.9		35.5	
Menopausal status	Premenopausal /Perimenopausal	12	22.2	0.45	31.5	0.72
	Postmenopausal	10	27.8		35.5	
Cardiovascular disease	+	7	29.2	0.16	31.6	0.53
	–	15	22.1		31.7	
Antihypertensive medication	+	3	34.0	0.21	51.2	0.39
	–	19	22.3		31.6	
Smoking	+	6	20.7	0.29	39.4	0.53
	–	16	28.2		30.0	
Lactation history	+	13	27.1	0.86	31.7	0.64
	–	8	24.5		43.2	
Body mass index	Unknown	1				
	< 25	16	27.8	0.44	39.5	0.10
	≥ 25	6	22.2		23.4	
Systolic blood pressure	< 130	15	19.3	0.02*	31.4	0.16
	≥ 130	7	34.00		51.2	
Hemoglobin (mg/dL)	< 13	5	34.7	0.63	43.6	0.07
	≥ 13	17	26.8		31.4	

Wilcoxon rank-sum test, \*p < 0.05. VBP, vessel branching point.

count.

In this study, whole-breast VBP counts per 100 cm<sup>2</sup> were evaluated and it was possible to obtain objective counts with high reproducibility. However, discrimination of arteries and veins on MRI was difficult, so we did not attempt to distinguish these vessels in the PAI analysis. There was a time difference of about 2 min between irradiating at one wavelength and irradiating with the other wavelength. Oxygen saturation could not be calculated accurately because of the slight body movement that occurs during breathing. It would be interesting to investigate oxygen saturation in further detail in the future if this problem can be solved.

We found that the mean VBP count decreased with increasing depth on both the affected and unaffected sides, suggesting that the imaging capability of PAI may decrease with increasing depth from the skin surface. Therefore, we opted to use a 7-mm depth from the skin surface for this study and acquired stable images.

Although more VBPs could be counted with PAI than with MRI, in this study, only VBPs on the blood vessel seen on MRI among the VBPs seen on PAI were counted. With the use of PAI images, the number of counted VBPs depends on the observer and can be affected by artifacts on PAI images. Therefore, we used MRI as the gold standard in order to eliminate interobserver differences.

The VBP count in the breast showed wide interindividual variation. Other than high systolic BP, we could not identify any parameter influencing the VBP count in the contralateral unaffected breast. The need for comparison with a contralateral unaffected breast when evaluating the number of VBPs limits the clinical application of this biomarker.

However, future technological advances in PAI will allow the acquisition of more data on fine vascular branching, such that VBP count can be obtained specifically for affected breasts without MRI. Due to the very large numbers and the accuracy of the measurements, an automated process is necessary. Furthermore, we still need to investigate interindividual differences in a larger group of patients and to clarify the changes in VBP count in relation to age and menopause by observing individuals over time.

When using the PAI-03 system, a laser with an output of several hundred millijoules was mounted to obtain a depth performance of at least 20 mm to identify cancer-related blood vessels. The findings of our present study suggest that it might be possible to use a weaker laser power for detection of VBPs in the subcutaneous superficial layer of the

breast. It may also be possible to perform PAI using light-emitting diodes [24].

Technologic advances in PAI have enabled us to acquire data on fine vascular branching and obtain VBP counts for the breast. Our preliminary research indicates that the VBP count is higher in breasts with cancer than in contralateral unaffected breasts. Although little is known about the mechanism involved, further investigations of VBPs using PAI are warranted to improve our understanding of the role of vascular networks within the breast, including in breast cancer, and for development of new diagnostic tools for primary breast cancer.

## 5. Conclusion

PAI enabled us to detect fine vascular characteristics, specifically, VBPs, in the breast. The VBP count in the subcutaneous superficial layer of the breast (up to 7 mm from the skin surface) appeared to be increased in breasts with cancer when compared with the contralateral breasts with no detectable cancer. Further research is needed to confirm these results.

## Conflict of interest

Yasufumi Asao, Toshifumi Fukui, and Takayuki Yagi are employees of Canon Inc., Japan. YA and TY were temporarily transferred to the Japan Science and Technology Agency for the duration of the study. Canon Inc. designed and invented the photoacoustic imaging system used in this study. The other authors have no conflict of interest.

## Acknowledgments

The authors wish to thank the patients who participated in this clinical study, T. Kosaka for coordinating the clinical research undertaken in this study, all members of Medical Imaging System Development Center, Canon Inc., for their technical support, and Canon Inc. for providing the PAI-03.

## Funding

This work is partially supported by the Innovative Techno-Hub for Integrated Medical Bio-imaging Project of the Special Coordination

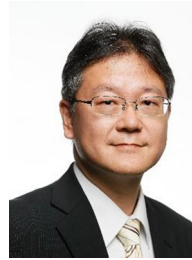
Funds for Promoting Science and Technology, from the Ministry of Education, Culture, Sports, Science, and Technology, Japan.

## References

- [1] J.R. Harris, M.E. Lippman, M. Morrow, C.K. Osborne, *Diseases of the Breast*, fourth ed., Lippincott Williams & Wilkins, Philadelphia, 2010.
- [2] D. Fukumura, D.G. Duda, L.L. Munn, R.K. Jain, Tumor microvasculature and microenvironment: novel insights through intravital imaging in pre-clinical models, *Microcirculation* 17 (2010) 206–225.
- [3] S. Kul, A. Cansu, E. Alha, H. Dinc, A. Reis, G. Çan, Contrast-enhanced MR angiography of the breast: evaluation of ipsilateral increased vascularity and adjacent vessel sign in the characterization of breast lesions, *AJR Am. J. Roentgenol.* 5 (2010) 1250–1254.
- [4] M. Toi, Y. Asao, Y. Matsumoto, H. Sekiguchi, A. Yoshikawa, M. Takada, M. Kataoka, T. Endo, N. Kawaaguchi-Sakita, M. Kawashima, E. Fakhrajahani, S. Kanao, I. Yamaga, Y. Nakayama, M. Tokiwa, M. Torii, T. Yagi, T. Sakurai, K. Togashi, T. Shiina, Visualization of tumor-related blood vessels in human breast by photoacoustic imaging system with a hemispherical detector array, *Sci. Rep.* 7 (2017) 41970.
- [5] H. Zhao, R. Xu, Q. Ouyang, L. Chen, B. Dong, Contrast-enhanced ultrasound is helpful in the differentiation of malignant and benign breast lesions, *Eur. J. Radiol.* 73 (2010) 288–293.
- [6] Q. Zhu, S. You, Y. Jiang, J. Zhang, M. Xiao, Q. Dai, Q. Sun, Detecting angiogenesis in breast tumors: comparison of color doppler flow imaging with ultrasound-guided diffuse optical tomography, *Ultrasound Med. Biol.* 37 (2011) 862–869.
- [7] S.A. Kostopoulos, K.G. Vassiou, E.N. Lavdas, D.A. Cavouras, I.K. Kalazis, P.A. Asvestas, D.L. Arvanitis, I.V. Fezoulidis, D.T. Glotsos, Computer-based automated estimation of breast vascularity and correlation with breast cancer in DCE-MRI images, *MRI* 35 (2017) 39–45.
- [8] W.R. Jia, W.M. Chai, L. Tang, Y. Wang, X.C. Fei, B.S. Han, M. Chen, Three-dimensional contrast enhanced ultrasound score and dynamin contrast-enhanced magnetic resonance imaging score in evaluating breast tumor angiogenesis: correlation with biological factors, *Eur. J. Radiol.* 9 (2014) 1098–1105.
- [9] O. Fernandez-Guinea, A. Andicochea, L.O. Gonzalez, S. Gonzalez-Reyes, A.M. Merino, L.C. Hernandez, A. Lopez-Muniz, P. Garcia-Pravia, F.J. Vizoso, Relationship between morphological features and kinetic patterns of enhancement of the dynamic breast magnetic resonance imaging and clinicopathological and biological factors in invasive breast cancer, *BMC Cancer* 10 (2010) 8.
- [10] B.J. Tromberg, B.W. Pongue, A.G. Yodh, D.A. Boas, A.E. Cerussi, Assessing the future of diffuse optical imaging technologies for breast cancer management, *Med. Phys.* 35 (2008) 2443–2451.
- [11] T. Kitai, M. Torii, T. Sugie, S. Kanao, T. Mikami, T. Shiina, M. Toi, Photoacoustic mammography: initial clinical results, *Breast Cancer* 21 (2014) 146–153.
- [12] E. Fakhrajahani, M. Torii, T. Kitai, S. Kanao, Y. Asao, Y. Hashizume, T. Mikami, I. Yamaga, M. Kataoka, T. Sugie, M. Takada, H. Haga, K. Togashi, T. Shiina, M. Toi, Clinical report on the first of a photoacoustic tomography system with dual illumination for breast cancer imaging, *PLoS One* 27 (2015) e0139113.
- [13] Y. Asao, Y. Hashizume, T. Suita, K. Ngai, K. Fukutani, S. Yoshiaki, T. Matsushita, S. Kobayashi, M. Tokiwa, I. Yamaga, E. Fakhrajahani, M. Torii, M. Kawashima, M. Takada, S. Kanao, M. Kataoka, T. Shiina, M. Toi, Photoacoustic mammography capable of simultaneously acquiring photoacoustic and ultrasound images, *J. Biomed. Opt.* 21 (2016) 116009.
- [14] R.T. Tong, Y. Boucher, S.V. Kozin, F. Winkler, D.J. Hicklin, R.K. Jain, Vascular normalization by vascular endothelial growth factor receptor 2 blockade induces a pressure gradient across the vasculature and improves drug penetration in tumors, *Cancer Res.* 64 (2004) 3731–3736.
- [15] R.A. Kruger, C.M. Kuzmiak, R.B. Lam, D.R. Reinecke, S.P. Del Rio, D. Steed, Dedicated 3D photoacoustic breast imaging, *Med. Phys.* 11 (2013) 113301.
- [16] M. Xu, L.V. Wang, Universal back-projection algorithm for photoacoustic computed tomography, *Phys. Rev. E Stat. Nonlin. Soft Matter Phys.* 71 (2005) 016706.
- [17] F.L. Bookstein, Principal warps: thin-plate splines and the decomposition of deformations, *IEEE Trans. Pattern Anal. Mach. Intell.* 11 (1989) 567–585.
- [18] L.P. Bos, K. Salkauskas, Moving least-squares are backus-gilbert optimal, *J. Approx. Theory* 59 (1989) 267–275.
- [19] M.J. Duffy, N. Harbock, M. Nap, R. Molina, A. Nicolini, E. Senkus, F. Cardoso, Clinical use of biomarkers in breast cancer: updated guidelines from the European group on tumor markers, *Eur. J. Cancer* 75 (2017) 284–298.
- [20] A.N. Mirza, N.Q. Mirza, G. Vlastos, S.E. Singletary, Prognostic factors in node-negative breast cancer, *Ann. Surg.* 235 (2002) 10–26.
- [21] S. Ueda, N. Nakamiya, K. Matsuura, T. Shigekawa, H. Sano, E. Hirokawa, H. Shimada, H. Suzuki, M. Oda, Y. Yamashita, O. Kishino, I. Kuji, A. Osaki, T. Saeki, Optical imaging of tumor vascularity associated with proliferation and glucose metabolism in early breast cancer: clinical application of total hemoglobin measurements in the breast, *BMC Cancer* 13 (2013) 514.
- [22] M. Torii, T. Fukui, M. Inoue, S. Kanao, K. Umetani, M. Shirai, T. Inagaki, H. Tsuchimochi, J.T. Pearson, M. Toi, Analysis of the microvascular morphology and hemodynamics of breast cancer in mice using Spring-8 synchrotron radiation microangiography, *J. Synchrotron Radiat.* 24 (2017) 1039–1047.
- [23] J.R. Less, M.C. Posner, Y. Boucher, N. Wolmark, R.K. Jain, Interstitial hypertension in human breast and colorectal tumors, *Cancer Res.* 52 (1992) 6371–6374.
- [24] A. Hariri, J. Lemaster, J. Wang, A.S. Jeevarathnam, D.L. Chao, J.V. Jokerst, The characterization of an economic and portable LED-based photoacoustic imaging system to facilitate molecular imaging, *Photoacoustics* 9 (2018) 10–20.



**Iku Yamaga** received her M.D. degree from Saga Medical College in 2003. She has been involved in the clinical study of Photoacoustic Mammography since 2012 at the department of Breast Surgery, Graduate School of Medicine, Kyoto University, and she has been working at the department of surgery in National Hospital Organization Kyoto Medical Center since 2016. She is focused on the clinical application of photoacoustic imaging for breast cancer.



**Yasufumi Asao** received his BS, MS, and PhD degrees in engineering from Tohoku University in 1991, 1993, and 2005, respectively. After serving as a manager of Canon Inc., and a research associate professor of Graduate School of Medicine, Kyoto University, he is currently in charge of promoting research activities as an associate program manager of the ImPACT Yagi program. He is the author of more than 10 journal articles. The current research theme is photoacoustic imaging and its clinical application.

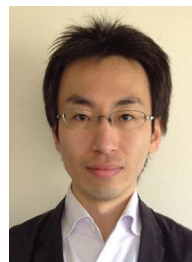


**Toshifumi Fukui** graduated at Keio University and received his B.A. degree in Environment and information in 1994. He has been working for Canon Inc. since 1994 as a data analyst and programmer. His specialty is computer science.



**Dr. Kataoka** graduated Faculty of Medicine, Kyoto University in 1996. Following her medical training, she received her PhD degree in Kyoto University Graduate School of Medicine in 2006. From 2006–2011, she worked as a research associate in the Department of Radiology, University of Cambridge and was involved in research in Breast imaging and Gynecologic imaging. Since 2011, she has been an assistant professor and also a group reader in breast imaging in Diagnostic Imaging and Nuclear Medicine, Kyoto University. She has also been involved in the project of photoacoustic mammography since 2011. Her role in the project is mainly about image evaluation and correlation with other imaging findings including Breast

MRI as a specialist in clinical diagnostic imaging.



**Masahiro Kawashima** is currently an assistant professor at Kyoto University in Japan. He graduated Faculty of Medicine and received his PhD degree from Graduate School of Medicine in Kyoto University. His research interests are the clinical management of breast cancer patients' care and the hypoxic responses of energy metabolism of breast cancer.



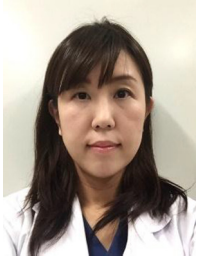


**Takayuki Yagi** was graduated and received master's degree from Graduate School of Interdisciplinary Science and Engineering, Tokyo Institute of Technology in 1983. He joined Canon INC in 1983 and has developed MEMS technologies and medical imaging technologies. One of medical imaging technologies was photoacoustic tomography. He was a Senior General Manager, Corporate R&D, Canon INC. after becoming Chief of Canon Research Center in 2005. He is presently a program manager of ImPACT which is a national prioritized project, established in the Cabinet Office in 2014. He is on transfer from Canon to ImPACT since 2014.



**Tsuyoshi Shiina** was graduated from the Electronic Engineering Department, the University of Tokyo, in 1982. He received PhD degrees in electronic engineering in 1987 from the University of Tokyo and the DMSC degree in 2006, from University of Tsukuba. From 1995 to 1996, he was with the institute of Cancer Research and the Royal Marsden NHS Trust in UK as Visiting Professor. He is presently a Professor of Human Health Sciences, Graduate School of Medicine, Kyoto University. His research interests include visualization technique of structural and functional bio-information and developed the practical ultrasound elastography for breast diagnosis in 2003. Recently, he involves the development of photoacoustic mammography as

the ImPACT program supported by Japanese government grant. He is vice-president of the Japan Society of Ultrasonics in Medicine.



**Mariko Tokiwa** was a graduate student in Breast Surgery Department, Graduate School of Medicine Kyoto University. She received her M.D. degree in 2007 from Kobe University. She has been working as a breast surgeon in Kobe City Medical Center General Hospital. Her research interests are the clinical application of photoacoustic imaging for breast cancer.



**Masakazu Toi** is a Professor of Breast Surgery at the Graduate School of Medicine at Kyoto University in Japan. He is involved in various innovative projects to develop new anticancer diagnostics and therapeutics, including biomarkers, bioimaging and antibody treatment, particularly related to breast cancer biology and treatment. He is a project leader of the Impulsing Paradigm Change through Disruptive Technologies Program (ImPACT) led by the Council for Science, Technology and Innovation (CSTI) of the Cabinet Office, Japan.



**Masae Torii** is a M.D. specializing in breast cancer. She has been doing research at the Department of Breast Surgery, Graduate School of Medicine, Kyoto University since 2011. Her major research interests are tumor vessel hemodynamics and hypoxia.